

C-terminal Truncation of p21^H Preserves Crucial Kinetic and Structural Properties*

(Received for publication, February 28, 1989)

Jacob John, Ilme Schlichting, Emile Schiltz‡, Paul Rösch, and Alfred Wittinghofer

From the Max-Planck-Institut für Medizinische Forschung, Abteilung Biophysik, Jahnstrasse 29, D-6900 Heidelberg 1, Federal Republic of Germany and the ‡Institut für Organische Chemie und Biochemie, Universität Freiburg, Albertstraße 21 D-7800 Freiburg, Federal Republic of Germany

The human c-Ha-ras protooncogene product p21^c was truncated at the C terminus by 23 amino acids. The resulting G-binding domain, p21(1-166) = p21^{c'}, can be crystallized as a complex with the slowly hydrolyzing GTP analogues guanosin-5'-[β,γ-imido]triphosphate, guanosin-5'-[β,γ-methylene]triphosphate, and guanosin-5'-O-(3-thiotriphosphate). We show here that this protein has biochemical properties very similar to those of the intact protein. Activating mutations in position 12 (Gly¹² → Val; Gly¹² → Arg) have the same effect on the properties of the truncated protein as on intact protein. Nuclear magnetic resonance (NMR) measurements show no apparent effect of the C-terminal deletion on the solution structure of p21. This suggests that neither the structure of the G-binding domain nor any of its biochemical properties are markedly influenced by the truncation.

p21 proteins are the products of the N-, K-, and Ha-ras genes. Single point mutations in these genes have been found in some acute transforming animal viruses and in a high percentage of human tumors. It appears that the mutations are involved in the development of these tumors. The corresponding mutated proteins have an amino acid substitution either at position 12/13 or 59/61 (for reviews see Refs. 1-3).

The p21 protein products of the Ha-, K-, and N-ras genes have identical amino acid sequences for the first 80 amino acids and are more than 85% identical up to amino acids 164/165. The C-terminal 25 amino acids are very divergent, except for the Cys-A-A-X-OH motif at the end of the chain (with A being an aliphatic residue). This motif has been shown to be responsible for anchoring the protein to the cell membrane (4-8). Due to their homology with other guanine nucleotide binding proteins, it is thought that p21 proteins function as signal-transducers. The yeast homologue of p21 (*Saccharomyces cerevisiae*) has indeed been shown to be involved in the activation of adenylate cyclase (9, 10). The function of p21 in higher eucaryotes is still a matter of intense research, and evidence is accumulating that p21 can effect the phosphatidylinositol signaling system (11, 12). All G proteins cycle between an "inactive" GDP- and an "active" GTP-conformational state (for reviews, see Refs. 13-15). The three-dimensional structure of the GDP complex of the G-binding domain, amino acids 1-171, of the p21^H protein has been determined by Kim and co-workers (16). We have recently crystallized the GppNp and the GppCp complexes of another

variant of the G domain, amino acids 1-166. The crystals of such complexes (Fig. 1) diffract to high resolution and the x-ray crystallographic determination of the three-dimensional structure of these complexes is currently being pursued in our laboratory (17). The three-dimensional structure should allow us to define the structural change during the GDP → GTP transition, which is the basis for the function of this and most likely all other G-binding proteins. It is, therefore, of great interest to clarify whether the properties of the G-binding domain reflect the properties of the complete protein. Here we show that the deletion of the C-terminal 23 amino acids from p21 does not influence the basic biochemical and structural properties of the G-binding domain.

MATERIALS AND METHODS

Cloning Techniques and Mutagenesis—Restriction endonucleases, T4 DNA Ligase, polynucleotide kinase, and dNTPs were from Boehringer Mannheim, Federal Republic of Germany. The above reagents were used as described in the laboratory manual of Maniatis *et al.* (18). Transformation was done according to the method of Hanahan (19) with frozen cells or according to the CaCl₂ method (18).

Site-directed mutagenesis was performed according to the method of Taylor and Eckstein (20), using *Xba*III from New England Biolabs and DNA polymerase (Klenow fragment) from Du Pont-New England Nuclear. Desoxycytidine-5'-O-(thiotriphosphate) was synthesized according to the method of Goody and Isakov (21). Briefly, the EcoRI-PstI fragment (680 base pairs) of the c-Ha-ras cDNA was cloned into M13mp9 and single strand DNA was prepared. The sequence of the oligonucleotide used for mutagenesis is: 5'-GG-CAG-CAC-TAG-CTG-CGG-3', whereby the stop codon TAG was introduced at codon 167. The introduction of this stop codon also leads to the creation of an *Mae*I restriction site, which was used in the initial screening for mutants. The DNA sequence of the mutated gene was verified by the dideoxy sequencing method (22). Following mutagenesis, the EcoRI-PstI fragment (680 base pairs) was cut out of M13mp9 and force-cloned into the expression vector ptac-ras32 (23). This plasmid is a modification of the previously described ptac-ras30 expression vector (24), in which the PstI restriction site in the β-lactamase gene and the EcoRI restriction site upstream from the "tac" promoter were removed, as described previously (23). The expression vector with the gene coding for truncated p21 is designated ptacrasC'. The mutations Gly¹² → Val¹² (G12V) and Gly¹² → Arg¹² (G12R) were introduced by substituting the 330-base pair EcoRI-NcoI fragment in ptacrasC' with the corresponding fragments from the plasmids ptacrasT (G12V) and ptacrasD (G12R), respectively, which express the full-length mutant proteins (23). The *Escherichia coli* strain CK600K was used as a host, which is K12 wild type CK600 containing the plasmid pDMI,1 (25) carrying the lac^r gene and a kanamycin resistance gene (K). This plasmid is compatible with the expression plasmids described here.

Protein Purification—Protein purification was performed essentially as described previously (24, 25), with the following modifications: the truncated proteins eluted from the Q-Sepharose column at a slightly higher sodium chloride concentration. Ammonium sulfate precipitation was done at 80% saturation with ammonium sulfate instead of 60%. The final purity of the proteins was 99%, as judged from sodium dodecyl sulfate-polyacrylamide gel electrophoresis. Pro-

* The costs of publication of this article were defrayed in part by the payment of page charges. This article must therefore be hereby marked "advertisement" in accordance with 18 U.S.C. Section 1734 solely to indicate this fact.

tein concentrations were determined with the Bradford assay (26) using bovine serum albumin as a standard, whereas [³H]GDP binding activity was determined by the filter binding assay (23, 24). Standard buffer was always, unless stated otherwise, 64 mM Tris-HCl, pH 7.6, 1 mM dithioerythritol, 10 mM MgCl₂ and 1 mM NaN₃.

Full-length p21 proteins which sometimes appeared as two bands of varying intensity on sodium dodecyl sulfate-polyacrylamide gels after purification were separated by hydrophobic interaction chromatography on a TSK-phenyl-5W column (27). The metal and nucleotide free p21 apoprotein fractions (full-length and 1-182 protein) thus obtained were immediately incubated with GDP and MgCl₂ in order to preserve their activity.

Sequencing of p21 Proteins—N-terminal Edman degradation was done by applying 50 μl of protein solution (approximately 1 mg/ml in 50 mM HEPES¹-NaOH, pH 7.5, 10 mM MgCl₂, 1 mM dithiothreitol, 1 mM NaN₃) to a pulsed liquid sequencer from Applied Biosystems, model 477A with 120A for on-line identification, following the directions of the company and Ref. 28). For C-terminal analysis the two different fractions from the HPLC separation on TSK-phenyl-5W (see "Protein Purification" section) were dialyzed against 1% acetic acid. 600 μg of lyophilized protein was dissolved in 300 μl of 0.1 M N-ethylmorpholine formate at pH 8.0. 30 μl of sodium dodecyl sulfate (10%), 1 μl of norleucin (10 mM), and 1 μl of a carboxypeptidase A suspension (25 mg/ml, Boehringer Mannheim) were added. 100-μl aliquots were removed after 0, 40, and 80 min at 37 °C. The digest was stopped with 20 μl of 0.4 M 5-sulfosalicylic acid and centrifuged at 15,000 × g for 5 min. 100 μl of the supernatant was used for amino acid analysis on a Biotronik BT 6000E amino acid analyzer.

Analytical Gel Filtration—Analytical gel filtration was carried out on an AcA54 column (Pharmacia LKB Biotechnology Inc., 91 × 1.6 cm) equilibrated with standard buffer containing 0.1 M NaCl and 10 mM β-mercaptoethanol. The void volume (V_0) of the column was determined as 64 ml using blue dextran (Pharmacia LKB Biotechnology Inc.). The elution volume (V_e) of the standard proteins and of p21 proteins were determined using solutions with different combinations of these proteins. The total volume (V_T) of the column was determined as 183 ml using a GMP solution. The column was developed at 18 ml/h at 20–23 °C. Standard proteins and their molecular masses in kilodaltons were: bovine serum albumin (67), ovalbumin (45), carbonic anhydrase (29), soybean trypsin inhibitor (22), and cytochrome c (12.5). The initial protein concentrations were 5–10 mg/ml.

GTPase Activity—GTPase activity measurements were essentially performed as described previously (23, 24). Briefly, p21·GDP (2 μM) was preincubated with [γ -³²P]GTP (40 μM) for 30 min at room temperature in a total volume of 1 ml in 1 mM EDTA, 64 mM Tris-HCl, pH 7.6, 2 mM dithioerythritol, 1 mM sodium azide. The concentration of MgCl₂ was brought to 10 mM and the temperature to 37 °C. 50-μl portions were removed at defined time intervals and the production of ³²P_i was measured as described.

Kinetics of Nucleotide Dissociation—The rate of dissociation of [³H]GDP from the p21·[³H]GDP complex was measured as described previously (23). All measurements were performed at 37 °C in standard buffer. Nitrocellulose filters from Sartorius (pore size = 0.1 μm) were used for the filter binding test, since the C-terminally truncated p21 did not bind quantitatively to nitrocellulose filters from other manufacturers. The reason for this is not known.

Inhibition of [³H]GDP Binding—The binding studies were performed as described previously (24), with minor modifications. Briefly, 1 μM p21·GDP was incubated with 9 μM [³H]GDP and varying concentrations of guanosine nucleotide analogues in a total volume of 100 μl in standard buffer with 1 mM EDTA at 0 °C until equilibrium was reached. 1 μl of 1 M MgCl₂ was added, and the mixture was incubated for 30 min. The probes were filtered, and the filter-bound radioactivity was determined.

Biological Activity of p21 in PC12 Cells—The pheochromocytoma cell line PC12 was grown under standard conditions with Dulbecco's

modified Eagle's medium supplemented with 10% horse serum, 5% fetal calf serum, and antibiotics (29). Approximately 5 × 10⁴ cells were collected by centrifugation in an Eppendorf tube. 40 μl of a protein solution containing 3 mg/ml p21 in standard buffer were added to the cells. The protein was introduced into the cytoplasm by pushing the cells through a yellow tip held at the bottom of the tube. This creates enough pressure such that the cell membrane is slightly ruptured and the protein enters the cell. This procedure has been described recently by us in detail (30). The cells were incubated again in standard medium in a petri dish, and neurite outgrowth was then monitored under the microscope.

NMR Sample Preparation—The proteins obtained after HPLC purification were concentrated by centrifugation in Centricon 10 microconcentrators (Amicon). H₂O was exchanged for D₂O by subsequent redilution with 50 mM D₂O sodium borate buffer. As shown under "Results," the spectra we obtained for the aromatic residues were identical whether or not we used HPLC to purify the protein. Therefore, we used the p21-GDP-Mg²⁺ complex as obtained from the normal protein preparation, which contains an estimated 10–20% p21(1-182), for the phosphorus and two-dimensional proton NMR experiments. These samples were dialyzed against sodium borate, potassium phosphate, or standard (Tris) buffer, freeze-dried, and redissolved in D₂O. The last two steps were repeated for proton NMR samples.

NMR Spectroscopy—NMR experiments were performed on a commercial Bruker AM 500 spectrometer working with a proton resonance frequency of 500 MHz and a phosphorus resonance frequency of 202 MHz. For the proton NMR experiments, 0.5-ml aliquots of sample in 5-mm sample tubes and a 5-mm probe were used, whereas 2.2-ml aliquots of sample in 10-mm sample tubes and a 10-mm probe were used for ³¹P spectroscopy. The proton spectra are referenced to internal sodium 2,2-dimethyl-2-silapentane-5-sulfonate, the phosphorous spectra to external 85% H₃PO₄. Sample temperature was kept at 303 K with a stream of dry air which was temperature-regulated with a standard Bruker VT1000 unit. The residual HDO resonance was suppressed by permanent (except acquisition) selective irradiation with the HDO frequency. Quadrature detection was used in all experiments. All two-dimensional experiments were performed in the phase-sensitive mode with the time proportional incrementation technique (31). For COSY and NOESY spectra usually 128 transients of 4000 data points were collected for each of 512 increments with a relaxation delay of 1.1 s between successive transients. The NOESY spectra were recorded with a mixing time of 0.15 s which was randomly varied by 15%. A sweep width of 4545.45 Hz was used in both dimensions. Prior to Fourier transformation apodization was carried out in both dimensions using an unshifted sine-bell filter for the double quantum-filtered COSY spectra and a π/32 shifted sine-bell filter for the NOESY spectra. The digital resolution was 8.9 Hz/point in t_1 after zero filling. Standard procedures and commercially available software on an Aspect 3000 computer were used throughout. In addition, for data evaluation a software package supplied in part by R. Kaptein, Utrecht, implemented in the C-programming language under the UNIX operating system on a Convex C210 computer was used.

RESULTS

p21(1-182) as a Side Product of p21 Expression in *E. coli*—A close inspection of some of the published polyacrylamide gels of bacterially expressed p21 seems to indicate the presence of two protein bands (e.g. Refs. 32, 33 and Footnote 2). We had also noted earlier (24) that p21 purified from bacterial extracts sometimes migrates on sodium dodecyl sulfate-polyacrylamide gels as two closely spaced bands. Often these bands cannot be separated and appear as one broad band on the gel. The amount of protein in the faster migrating band depends on bacterial growth and protein purification conditions. It seems to be higher for viral p21(G12R, A59T) and other transforming forms of the protein. We were able to separate these bands by the HPLC method which we developed earlier to prepare nucleotide and metal ion free p21 (27). The two protein bands are well separated after the HPLC procedure (data not shown). Both fractions were subjected to N- and C-

¹ The abbreviations used are: HEPES, 4-(2-hydroxyethyl)-1-piperazineethanesulfonic acid; p21_c, the protein product of the human c-Ha-ras protooncogene; p21_{c'}, the C-terminally truncated version of the above protein comprising amino acids 1-166; GppCp, guanosin-5'-[β,γ-methylene]triphosphate; GppNp, guanosin-5'-[β,γ-imido]triphosphate; GTPγS, guanosin-5'-O-(3-thiotriphosphate); dCTPαS, desoxycytidine-5'-O-(thiotriphosphate); NMR, nuclear magnetic resonance; HDO, hydrogen deuterium oxide; COSY, correlated spectroscopy; NOESY, nuclear Overhauser enhancement spectroscopy; HPLC, high performance liquid chromatography.

² A. Hall and P. Lowe, personal communications.

terminal protein sequence determination. Edman degradation showed that both proteins contained the N-terminal sequence Met-Thr-Glu-Tyr-Lys-Leu-Val expected from the native p21 proteins. It should be mentioned, however, that the protein preparations contained varying amounts of an isomer which had lost the N-terminal methionine. In the case of the full-length protein, this amounted to 20% in one sample, and truncated p21 contained 10% of this form. Carboxypeptidase digestion of each protein fraction showed that the C termini were different: whereas the slower migrating protein contained the expected amino acids at the C terminus, the faster migrating protein ended with methionine. Since only methionine 182 is situated near the C terminus, this shows that the lower band is p21(1-182), where seven amino acids have been deleted, presumably by proteolysis in *E. coli*. The p21(1-182) showed full activity in the binding of [8-³H]GDP, and its structural properties seemed to be undistinguishable from native p21 as evidenced by NMR spectroscopy (see below). Since we were not able to crystallize this protein, we did not investigate its biochemical properties further.

Mutation and Expression of the G Domain p21(1-166)—The alignment of the primary sequences of the three different ras genes from mammalian sources and the ras genes from lower eucaryotes shows that the high sequence homology of these genes breaks down in the region of amino acids 164–165. We thus mutated the conveniently located Lys¹⁶⁷ codon AAG to the stop codon TAG. The truncated version of the protein p21(1-166), termed p21_{C'}, was expressed in high yields using the expression vector ptacrasC' which is similar to ptacras32 described before (Ref. 24, see also "Materials and Methods"). The protein was purified by the same two-step purification scheme that has been described elsewhere (23, 24), with minor modifications.

For the expression of the Gly¹² → Val (G12V), Gly¹² → Arg (G12R) mutants of p21_{C'} the EcoRI-NcoI fragment from ptacrasT and ptacrasD, which express the mutated versions of the protein (23), were inserted into ptacrasC'. These proteins were purified according to identical purification schemes. All isolated p21 proteins bind radiolabeled GDP with ~90% of the theoretical maximum. Fig. 1 shows that the truncated p21_{C'} can be crystallized as the GppNp as well as the GppCp complex. The crystals of the GppNp complex are of high stability and diffract x-rays to high resolution. They are currently being analyzed to reveal conformational transitions between the GDP and the GTP bound form of the protein.

It should be noted that the truncated p21 proteins did not bind efficiently to the commonly used nitrocellulose filters with a pore size of 0.45 μm. However, they do bind to nitrocellulose filters with 0.1-μm pore size, albeit not from all suppliers. This is in line with the observation that in cellular extracts from brain and other tissues the small G-binding protein (M_r 20,000–25,000) can be blotted much more efficiently with nitrocellulose filters with pore size ≤0.2 μm.³

Analytical Gel Filtration—It was reported recently that p21 proteins show a tendency for homooligomeric structure (34). We also found indications that p21 does not behave as a monomeric protein. In order to find out whether the C terminus is involved in this property of the protein, we determined the molecular weight of normal and truncated p21 by gel filtration analysis using an AcA54 column, as shown in Fig. 2. We find that normal p21 runs as a single symmetric peak corresponding to an apparent molecular mass of 25 kDa, which is 20% higher than the calculated molecular mass of the monomer. Truncated p21, however, has an elution volume

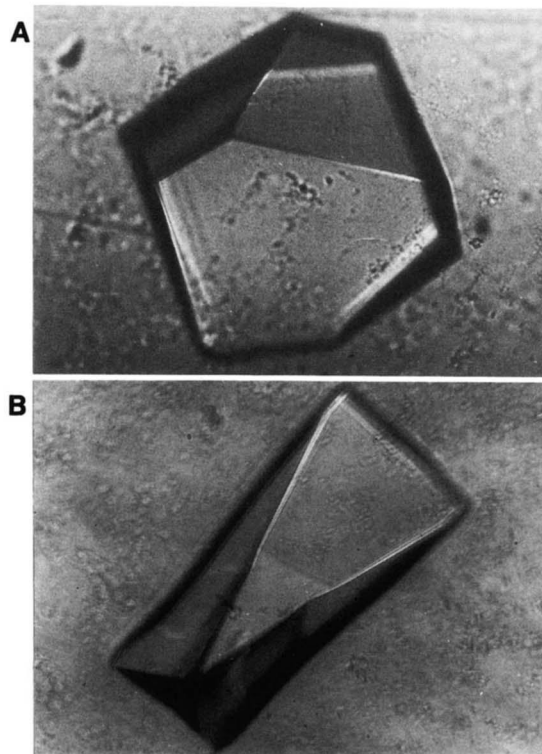


FIG. 1. Crystals of the p21_{C'} protein complexed to GppNp (A) and GppCp (B) in the presence of Mg²⁺. Both crystals are shown at the same magnification. They were grown using polyethylene glycol (PEG 1450) in standard buffer and are approximately 300 (GppNp) and 400 μm (GppCp) along the longest axis.

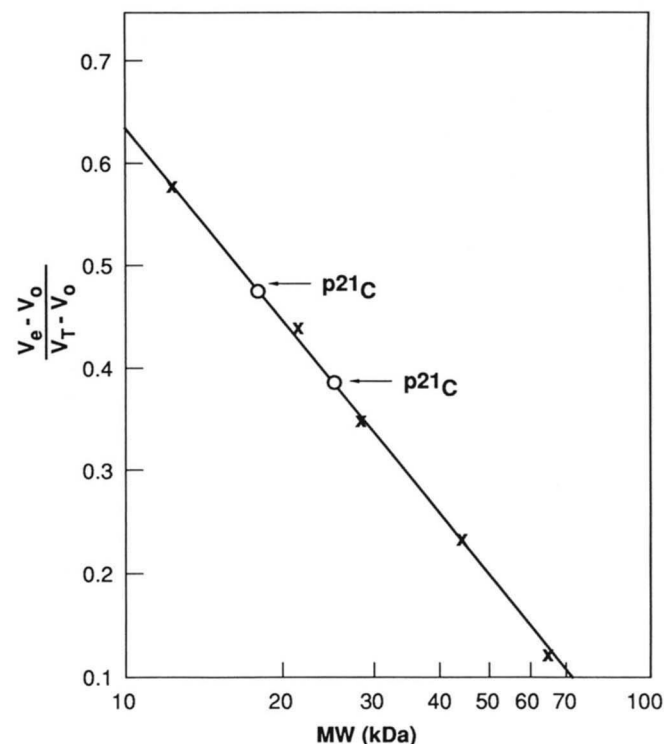


FIG. 2. Gel filtration analysis of normal and truncated p21. A calibration curve for various standard proteins on a gel filtration column of AcA54 (1.6 × 91 cm) was prepared using the standard proteins as described under "Materials and Methods." The elution volumes of p21_{C'} and p21_C were measured on this column and used to determine the apparent molecular weights of these proteins.

³ R. Schmitt, personal communication.

on the column that corresponds exactly to its calculated molecular mass of 18.5 kDa.

Biochemical Properties—We have shown earlier that the mutation of Gly¹² to Val or Arg leads to a 2- to 4-fold decrease in the GDP dissociation rate constant of p21 (23). Table I shows the results of the dissociation rate constant measurements for p21_{C'} and p21' (G12V). The truncated cellular p21 shows the same GDP dissociation rate constant as the intact cellular p21, *i.e.* $7.9 \times 10^{-3} \text{ min}^{-1}$. The rate is decreased to $3.3 \times 10^{-3} \text{ min}^{-1}$ by the Gly¹² → Val mutation. The decrease is thus 2.4-fold, somewhat smaller than with intact p21 (3.6-fold). The association rate constants of truncated p21 with guanosine nucleotides could not be determined by the filter binding method (35), since the filters used (Sartorius, 0.1-μm pore size) have a filtration time of almost 1 min. This is far too slow for rapid kinetic measurements.

It has been observed by many authors that the main biochemical consequence of the transforming mutation in Gly¹² is the decrease of the *in vitro* GTPase reaction rate (36–39). We have measured the GTP hydrolysis reaction for the truncated proteins (Table I). The rate constant for GTP hydrolysis is 0.037 min^{-1} for p21_{C'}, very similar to what we have found for intact protein under the same conditions. Again, as for the intact protein, mutations in the Gly¹² position lead to an approximately 10-fold decrease of the reaction rate. p21'(G12V) has a GTPase rate of $3.1 \times 10^{-3} \text{ min}^{-1}$ and p21'(G12R) of $3.6 \times 10^{-3} \text{ min}^{-1}$.

We also determined the affinities of GTP and GTP analogues relative to GDP by measuring the inhibition of [³H]GDP binding in the presence of increasing concentrations of nucleoside triphosphates (24). For p21_{C'} and p21_C the relative order of affinities is GTP > GDP > GTPγS > GppNp > GppCp (Table II). The relative order of nucleotide affinities for p21(G12V), and its truncated form is GDP > GTP > GTPγS > GppNp > GppCp which is in accord with our earlier observation that several activating mutations of p21 in position 12 and 59/61 reverse the relative affinity of GDP and GTP. The largest difference in nucleotide affinities between normal and truncated p21 is found for GTP.

Biological Properties—It has been shown before that microinjected p21 proteins with mutations in position Gly¹² and

TABLE I
GDP dissociation and GTPase rate constants of p21 proteins measured in standard buffer at 37 °C as described under "Materials and Methods"

Protein	GDP dissociation	GTP hydrolysis
	$k_{-4} \times 10^3 \text{ min}^{-1}$	$k_2 \times 10^3 \text{ min}^{-1}$
p21 _C	7.9	28
p21 _{C'}	7.8	37
p21(G12V)	2.3	3.8
p21'(G12V)	3.3	3.1
p21'(G21R)	ND ^b	3.6

^a k_2 is the rate constant for the true GTP cleavage step.

^b ND, not determined.

TABLE II
Affinities of GTP and GTP analogs relative to GDP, measured by the inhibition of [³H]GDP binding as described under "Materials and Methods"

Protein	Nucleoside triphosphate			
	GTP	GTPγS	GppNp	GppCp
p21 _C	1.9	0.72	0.09	0.01
p21 _{C'}	1.1	0.3	0.07	0.01
p21(G12V)	0.67	0.37	0.035	0.0036
p21'(G12V)	0.7	0.18	0.03	0.003

Gln⁶¹ transform fibroblasts in cell culture (40, 41). Microinjection of these proteins also induces the rat pheochromocytoma cell line PC12 to produce neurite fibers, thus mimicking the effect of nerve growth factor, which seems to suggest that p21 is involved in the signal-transducing pathway of the factor (42). Fig. 3A shows the result of such an experiment where p21(G12V) has been pressure-loaded (30) into PC12 cells. After 60 h the effect of the protein on differentiation has reached a maximum. This effect cannot be observed with the truncated form of the protein p21'(G12V), Fig. 3B. This confirms the absolute necessity of the C terminus for the biological function of p21.

NMR Investigations—We reported earlier that in the phosphorus NMR spectra of p21-guanine nucleotide complexes the β-phosphates of the p21·GDP·Mg²⁺ and p21·GTP·Mg²⁺ complexes experience a chemical shift change of 4 and 4.6 ppm, respectively, in downfield direction on complexation (43). The ³¹P NMR spectra of the native and truncated forms of p21_C·GDP·Mg²⁺ are virtually identical (Fig. 4), suggesting similar local environments of the enzyme-bound phosphates. Thus, we conclude that the C-terminal deletion does not perturb the binding site of either phosphate group.

Although the line widths of the proton NMR spectra of p21 are generally quite large and the resonances overlap strongly (Fig. 5), NMR is still useful for comparisons of the overall structures of different forms of p21. The presence of the high field shifted methyl proton resonances around 0 ppm indicates a well defined tertiary structure of full-length and truncated forms of p21 as obtained from our preparations. The spectra of p21_C and p21(1–182) (seven amino acids deleted) differ somewhat in the aliphatic region around 1–2 ppm, whereas the part of the spectrum resulting from the protons in aromatic side chains (6–9 ppm, Fig. 5) and the high field shifted

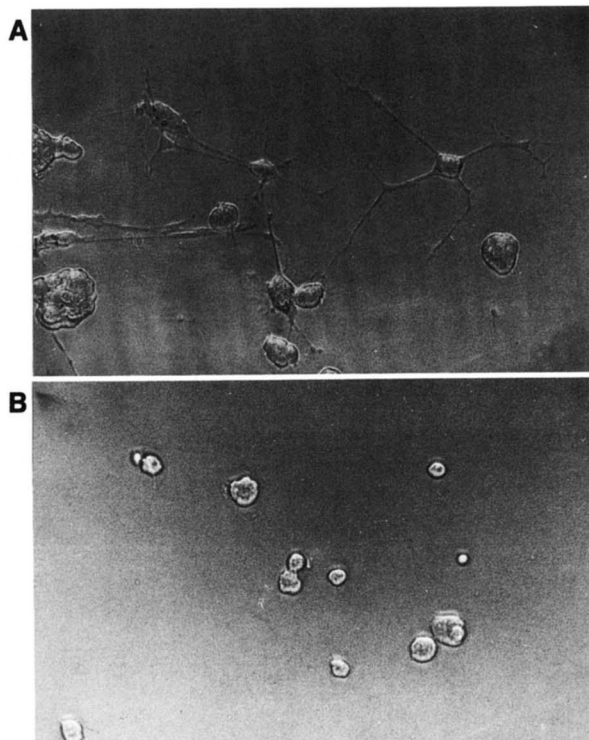


FIG. 3. Effect of normal and truncated p21(G12V) on PC12 cells. The rat pheochromocytoma cell line PC12 was loaded with p21 protein as described under "Materials and Methods" and Ref. 30. The cells were incubated for 60 h in standard medium in a Petri dish, and a typical area was photographed under phase contrast conditions. A, p21(G12V), full-length. B, p21'(G12V), truncated.

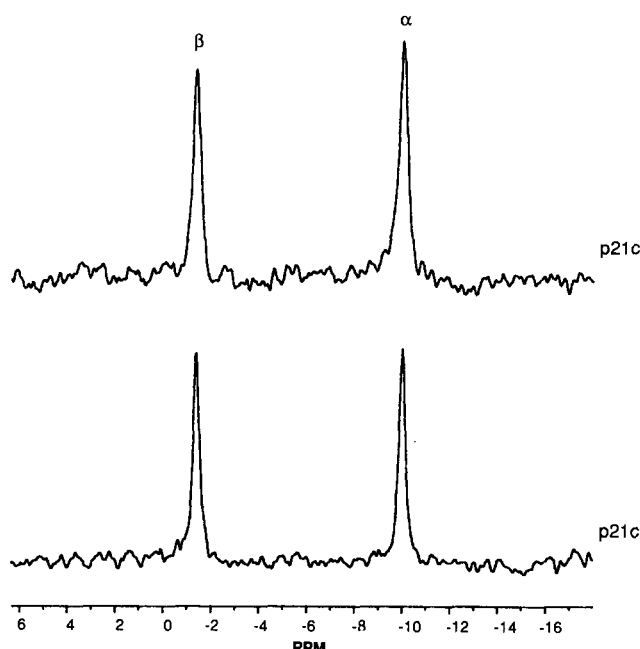


FIG. 4. ^{31}P NMR spectra of 1 mM Mg^{2+} -GDP complexes of p21_C and $\text{p21}_\text{C}'$ in 64 mM Tris-HCl, pH 7.6, 10 mM MgCl_2 , 8 mM dithioerythritol, 1 mM NaN_3 .

methyl proton resonances around 0 ppm are virtually identical. We can conclude from this that the tertiary structures of p21_C and $\text{p21}(1-182)$ are nearly identical. Similarly, only marginal differences can be found for the high field methyl proton region as well as the aromatic side chain protons in the spectra of p21_C and $\text{p21}_\text{C}'$ (Fig. 5).

We have investigated the aromatic region of the p21 ^1H NMR spectra and were able to identify and partly assign most of the aromatic spin systems of the protein.⁴ Apart from changes in the chemical shift values of the histidine imidazole proton resonances, no pH-dependent effects on p21_C and $\text{p21}_\text{C}'$ NMR spectra could be observed in the range pH 6.6–8.0. Fig. 6 shows in comparison the double quantum-filtered spectra of the Mg^{2+} -GDP complexes of p21_C and $\text{p21}_\text{C}'$. No severe differences could be detected apart from one additional set of tyrosyl ring resonances (6.92/7.0 ppm) appearing in the spectrum of $\text{p21}_\text{C}'$. Due to the severe overlap of resonance lines in the region of the aliphatic side chain proton resonances, this part of the spectra could not be compared in such detail. We conclude again that the structures of p21_C and $\text{p21}_\text{C}'$ are highly similar.

In order to obtain spatial information on the location of the GDP in the p21_C -GDP- Mg^{2+} and $\text{p21}_\text{C}'$ -GDP- Mg^{2+} complexes, we recorded NOESY spectra of these complexes. The intensity of NOESY cross-peaks is proportional to the inverse sixth power of the mutual distances of dipolar (through space) coupled protons. These cross-peak intensities are thus very sensitive indicators of proton-proton distances. It is generally agreed on that 0.5 nm is the upper distance limit between protons showing NOESY cross-peaks under the usual experimental conditions (44). We found a number of NOESY cross-peaks that are potentially useful for a more detailed structural analysis of p21 , e.g. NOESY cross-peaks between the resonances of the C1'-H of the ribose of the bound GDP at 6.09 ppm and the resonances belonging to the aromatic ring of Phe²⁸ at 6.51 and 6.69 ppm could be identified.⁴ These NOESY

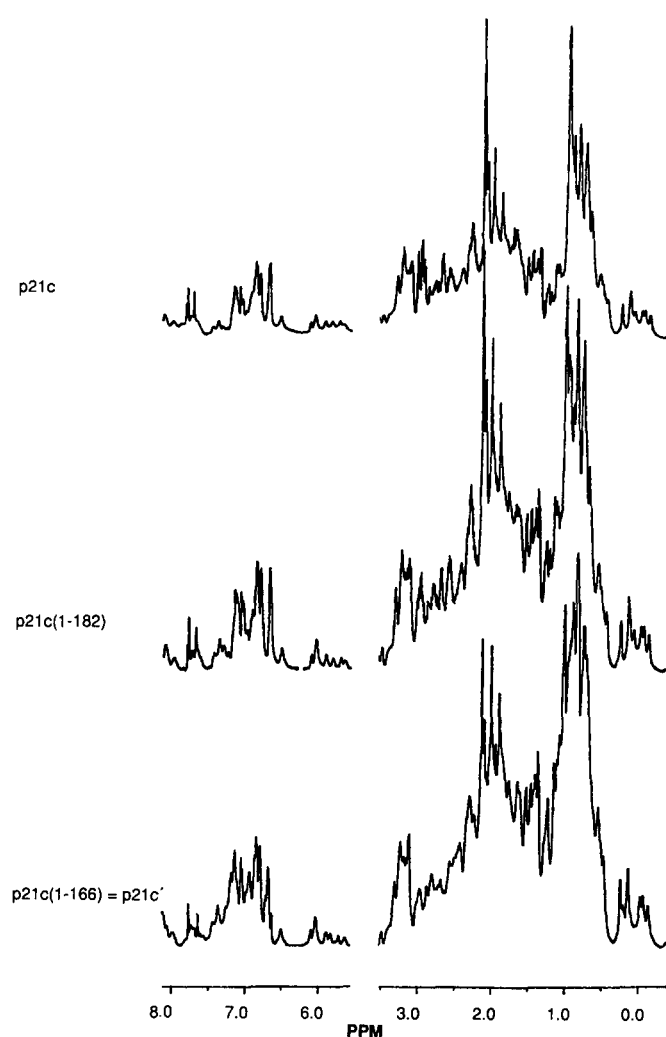


FIG. 5. ^1H NMR spectra of normal and two different truncated forms of p21_C . The spectra shown are from 2.9 mM p21_C , 1 mM $\text{p21}_\text{C}(1-182)$, and 3.5 mM $\text{p21}_\text{C}'$, all as protein-GDP- Mg^{2+} complexes in 50 mM sodium borate buffer, pH 8.0, 10 mM MgCl_2 , 3 mM dithioerythritol, 1 mM NaN_3 .

cross-peaks are identical in p21_C and $\text{p21}_\text{C}'$ as shown in Fig. 7.

DISCUSSION

It has been shown that the C terminus of p21 is involved in the posttranslational processing of the molecule and is required for its biological activity (4–8). This is in line with our observation that the deletion of 25 amino acids from the C terminus of the transforming mutant $\text{p21}(G12V)$ destroys the capacity of the protein to induce neurite outgrowth of PC12 cells or to promote survival of chick embryonic neurons after pressure-loading the cells with this protein (30).

We also find that the C-terminal truncation modifies certain properties of the protein that may be related to its hydrophobicity. It reduces the ability of the protein to bind to certain nitrocellulose filters, as well as its tendency to form oligomers. The latter is indicated by the difference between the observed and theoretical molecular weight of the full-length protein. No such difference was observed for the truncated proteins. $\text{p21}_\text{C}'$ is very different from p21_C in its ability to crystallize, since we have so far not been able to crystallize the complete protein complexed to any GTP analogue. However, other biochemical and structural properties of the trun-

⁴ I. Schlichting, J. John, M. Frech, P. Chardin, A. Wittinghofer, H. Zimmerman, and P. Rösch, *Biochemistry*, submitted for publication.

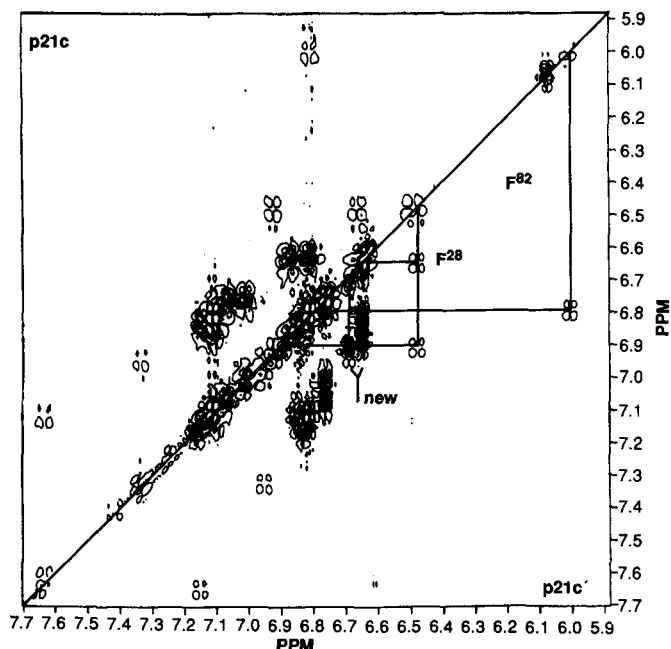


FIG. 6. COSY spectra of 3.2 mM p21_c (buffer: 50 mM potassium phosphate, pH 6.5, 50 mM MgCl₂, 6 mM dithioerythritol, 3 mM NaN₃) and 3.5 mM p21_{c'} as Mg²⁺·GDP complexes (buffer: 30 mM sodium borate buffer, pH 8.0, 6 mM MgCl₂, 6 mM DTE, 1 mM NaN₃). Only the aromatic portion of the spectra is shown.

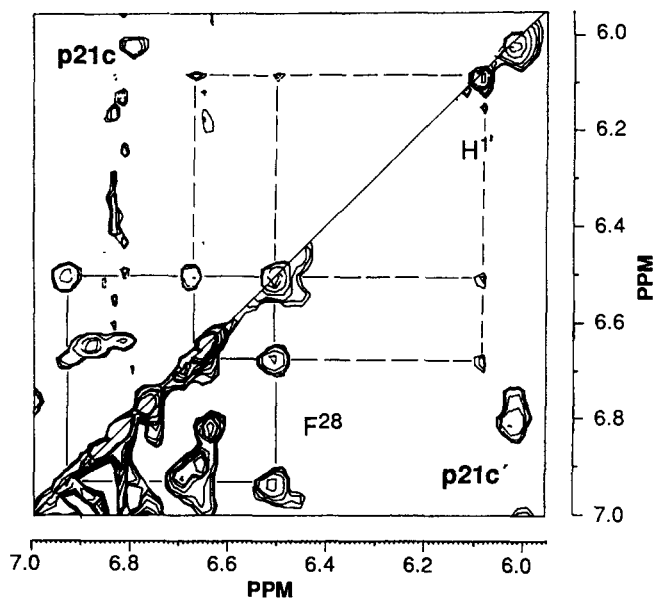


FIG. 7. NOESY spectra of 3.7 mM p21_c and 3.6 mM p21_{c'} as Mg²⁺·GDP complexes in 30 mM potassium phosphate buffer, pH 6.6, 30 mM MgCl₂, 6 mM dithioerythritol, 3 mM NaN₃.

cated proteins are only marginally altered in the truncated protein. They retain the ability to bind GDP stoichiometrically with a high binding constant, that is estimated to be also $>10^{10}$ mol⁻¹, as we have found for intact p21 (35). This is based on the fact that the dissociation rates are very similar if not identical and on the assumption that the association rate constants are close to the values found for full-length proteins. The GTPase rates of normal and truncated proteins are very similar. In addition, the C-terminal deletion preserves the effect of the Gly¹² → Val mutation which leads to a

reduction of the GTPase and GDP dissociation rate constants and changes the relative affinities of GTP and GDP.

NMR spectra of p21_c and p21_{c'} show that the overall structures of the molecules are preserved and that certain characteristic features of the spectra are identical for the two proteins. In particular, the structures of the p21_c·GDP·Mg²⁺ and the corresponding p21_{c'} complex are most likely identical around the phosphate groups as shown by ³¹P NMR and around the ribose moiety as evidenced by the identical ribose Cl'-H/Phe²⁸ cross-peaks in the NOESY spectra. This NOESY cross-peak is in accordance with the three-dimensional crystal structure determined by DeVos *et al.* (16), which shows Phe²⁸ situated perpendicular to the guanine base. The aromatic side chains are distributed rather evenly along the protein sequence. Since the region of resonances from the aromatic side chain protons is virtually identical for the two proteins even in the COSY and NOESY spectra of p21_c·GDP·Mg²⁺ and p21_{c'}·GDP·Mg²⁺, it may safely be concluded that both proteins have highly similar structures.

Thus, we feel safe to suggest that conclusions drawn from studies of the nucleotide complexes of the truncated p21(1–166) are in general also valid for the wild type protein as long as nothing is concluded about protein-protein or membrane-protein interactions via the C terminus. The crystal structure determination of the triphosphate complex of p21(1–166) should thus allow us, in combination with the three-dimensional structure of the GDP complex (16), to define the transition between the "signal-off" (= GDP, inactive) and the "signal-on" (= GTP, active) state of the protein. These conclusions should also be valid to define similar structural and functional transitions of other G-binding proteins.

Acknowledgments—We thank Anna Scherer and Peter Lang for technical assistance, Gian Borasio and Hans-Jörg Rindt for teaching us the pressure-loading technique, Roger S. Goody for nucleotide analogues, and Kenneth C. Holmes for continuous support.

REFERENCES

- Gibbs, J. B., Sigal, I. S., and Scolnick, E. M. (1985) *Trends Biochem. Sci.* **10**, 350–353
- Shih, T., Hattori, S., Clanton, D. J., Ulsh, L. S., Che, Z.-Q., Lautenberger, J. A., and Papas, T. S. (1986) in *Gene Amplification and Analysis* (Papas, T. S. and VandeWoude, G. F., eds) Elsevier Scientific Publishing Co., Inc., New York
- Barbacid, M. (1987) *Annu. Rev. Biochem.* **56**, 779–827
- Willumsen, B. M., Christensen, A., Hubbert, N. L., Papageorge, A. G., and Lowy, D. R. (1984) *Nature* **310**, 583–586
- Sefton, B. M., Trowbridge, I. S., Cooper, J. A., and Scolnick, E. M. (1982) *Cell* **31**, 465–474
- Chen, Z.-Q., Ulsh, L. S., DuBois, G., and Shih, T. Y. (1985) *J. Virol.* **56**, 607–612
- Buss, J. E., and Sefton, B. M. (1986) *Mol. Cell. Biol.* **6**, 116–122
- Fujiyama, A., and Tamanoi, F. (1986) *Proc. Natl. Acad. Sci. U. S. A.* **83**, 1266–1270
- Toda, T., Uno, I., Ishikawa, T., Powers, S., Kataoka, T., Broek, D., Cameron, S., Broach, J., Matsumoto, K., and Wigler, M. (1985) *Cell* **40**, 27–36
- Broek, D., Samiy, N., Fasano, O., Fujiyama, A., Tamanoi, F., Northup, J., and Wigler, M. (1985) *Cell* **41**, 763–769
- Hannock, J. F., Marshall, C. J., McKay, I. A., Gardner, S., Houslay, M. D., Hall, A., and Wakelam, M. J. O. (1988) *Oncogene* **3**, 187–193
- Fleischmann, L. F., Chawalla, S. B., and Cantley, L. (1986) *Science* **231**, 407–410
- Kaziro, Y. (1978) *Biochim. Biophys. Acta* **505**, 95–127
- Gilman, A. G. (1984) *Cell* **36**, 577–579
- Stryer, L., and Bourne, H. R. (1986) *Ann. Rev. Cell Biol.* **2**, 391–419
- DeVos, A., Tong, L., Milburn, M. V., Matias, P. M., Jancarik, J., Noguchi, S., Nishimura, S., Miura, K., Ohtsuka, E., and Kim, S.-H. (1988) *Science* **239**, 888–893
- Scherer, A., John, J., Linke, R., Goody, R. S., Wittinghofer, A.,

- Pai, E. F., and Holmes, K. C. (1989) *J. Mol. Biol.* **206**, 257–259
18. Maniatis, T., Fritsch, E. F., and Sambrook, J. (1982) *Molecular Cloning: A Laboratory Manual*, Cold Spring Harbor Laboratory, Cold Spring Harbor, NY
19. Hanahan, D. (1983) *J. Mol. Biol.* **166**, 557–580
20. Taylor, J. W., Ott, J., and Eckstein, F. (1985) *Nucleic Acids Res.* **13**, 8765–8785
21. Goody, R. S., and Isakov, M. (1986) *Tetrahedron Lett.* **27**, 3599–3602
22. Sanger, F., Nicklen, S., and Coulson, A. R. (1977) *Proc. Natl. Acad. Sci. U. S. A.* **74**, 5463–5467
23. John, J., Frech, M., and Wittinghofer, A. (1988) *J. Biol. Chem.* **263**, 11792–11799
24. Tucker, J., Sczakiel, G., Feuerstein, J., John, J., Goody, R. S., and Wittinghofer, A. (1986) *EMBO J.* **5**, 1351–1358
25. Certa, U., Bannwarth, W., Stüber, D., Gentz, R., Lanzer, M., LeGrice, S., Guillot, G., Wendler, I., Hunsmann, G., Bujard, H., and Mous, J. (1986) *EMBO J.* **5**, 3051–3956
26. Bradford, M. M. (1976) *Anal. Biochem.* **72**, 248–254
27. Feuerstein, J., Goody, R. S., and Wittinghofer, A. (1987) *J. Biol. Chem.* **262**, 8455–8458
28. Hunkapiller, M. W., Hewick, R. M., Dryer, W. J., and Hood, L. E. (1983) *Methods Enzymol.* **91**, 399–413
29. Greene, L. A., and Tischler, A. T. (1982) *Adv. Cell. Neurobiology* **3**, 373–414
30. Borasio, G. D., John, J., Wittinghofer, A., Barde, Y.-A., Sendtner, M., and Heumann, R. (1989) *Neuron* **2**, 1087–1096
31. Marion, D., and Wüthrich, K. (1983) *Biochem. Biophys. Res. Commun.* **113**, 967–974
32. Clark, R., Wong, G., Arnhem, N., Nitecki, D., and McCormick, F. (1985) *Proc. Natl. Acad. Sci. U. S. A.* **82**, 5280–5284
33. Manne, V., Yamazaki, S., and Kung, H.-F. (1984) *Proc. Natl. Acad. Sci. U. S. A.* **81**, 6953–6957
34. Santos, E., Nebreda, A. R., Bryan, T., and Kempner, E. S. (1988) *J. Biol. Chem.* **263**, 9853–9858
35. Feuerstein, J., Kalbitzer, H. R., John, J., Goody, R. S., and Wittinghofer, A. (1987) *Eur. J. Biochem.* **162**, 49–55
36. McGrath, J. P., Capon, D. J., Goeddel, D. V., and Levinson, A. D. (1984) *Nature* **310**, 644–649
37. Gibbs, J. B., Sigal, I. S., Poe, M., and Scolnick, E. M. (1984) *Proc. Natl. Acad. Sci. U. S. A.* **81**, 5704–5708
38. Sweet, R. W., Yokoyama, S., Kamata, T., Feramisco, J. R., Rosenberg, M., and Gross, M. (1984) *Nature* **311**, 273–275
39. Manne, V., Bekesi, E., and Kung, H.-F. (1985) *Proc. Natl. Acad. Sci. U. S. A.* **82**, 376–380
40. Feramisco, J. R., Gross, M., Kamata, T., Rosenberg, M., and Sweet, R. W. (1984) *Cell* **38**, 109–117
41. Stacey, D. W., and Kung, H.-F. (1984) *Nature* **310**, 503–511
42. Bar-Sagi, D., and Feramisco, J. R. (1985) *Cell* **42**, 841–848
43. Rösch, P., Wittinghofer, A., Tucker, J., Sczakiel, G., Leberman, R., and Schlichting, I. (1986) *Biochem. Biophys. Res. Commun.* **135**, 549–555
44. Wüthrich, K. (1986) *NMR of Proteins and Nucleic Acids*, John Wiley and Sons, New York